ELSEVIER

Journal of Structural Geology 26 (2004) 1419–1424

JOURNAL OF STRUCTURAL GEOLOGY

www.elsevier.com/locate/jsg

Clast-size analysis of impact-generated pseudotachylite from Vredefort Dome, South Africa

Eiko Hisada*

[a]*Department of Geology, Rand Afrikaans University, P.O. Box 524, Auckland Park 2006, South Africa*

Received 19 March 2002; received in revised form 14 March 2003; accepted 31 October 2003

Available online 11 March 2004

Abstract

Clast sizes in pseudotachylite from Vredefort Dome, South Africa, which is generally regarded as being of impact-origin, were studied. Clast-size analyses were conducted on the outcrop and thin section scales, and the clast-size distribution is fractal on each scale. On the outcrop scale, the clast-size distribution of the impact-generated pseudotachylite has a small D-value ($D = 1.29 \pm 0.02$). On the thin section scale, the D-values ($D = 1.68 \pm 0.22$ and 1.85 ± 0.13) may be slightly larger than those of fault-generated pseudotachylites and natural fault gouge, and a probable lower fractal limit (≈ 50 μm) is on the same order as that for fault-generated pseudotachylites. On the thin section scale, proportion of clasts for the impact-generated pseudotachylites is larger than that for fault-generated pseudotachylites, and on the outcrop scale, the impact-generated pseudotachylite has a remarkably high proportion of clasts.

Keywords: Pseudotachylite; Clast-size analysis; Fractal; Vredefort Dome

1. Introduction

Pseudotachylite is a cohesive glassy or very fine-grained rock, and it has been reported in many fault and shear zones (e.g. Sibson, 1975; Passchier, 1982), and in impact structures (e.g. Lambert, 1981; Reimold et al., 1987). With regard to the origin of fault-generated pseudotachylite, clast-size distribution has been studied by a number of authors (Shimamoto and Nagahama, 1992; Nagahama et al., 1994; Okamoto and Kitamura, 1994; Ray, 1999). They fitted power-laws to the size distributions of clasts and concluded that the major part of the matrix of these pseudotachylites cannot be explained by cataclasis alone and that both cataclasis and fusion may coexist in the pseudotachylite. Tsutsumi (1999) produced synthetic pseudotachylite by high-velocity frictional experiments and showed that the size distribution of clasts in the experimental pseudotachylite obeys a power-law that has been recognized in natural pseudotachylite.

Concerning impact-generated pseudotachylite, many workers agree that large-scale pseudotachylite is formed by the movement of basement blocks during the later stages of the cratering event (Dence et al., 1977; Lambert, 1981; Thompson and Spray, 1994; Spray and Thompson, 1995). However, unambiguous criteria for comparison and distinction of fault- and impact-generated pseudotachylites have not been identified yet (Reimold, 1995, 1998). Despite numerous studies on the mineralogy, chronology and chemistry of impact-generated pseudotachylites, few studies have attempted to understand the formation of the pseudotachylites from the viewpoint of clasts contained in the matrix. Size distributions and proportion of the clasts in the impact-generated pseudotachylite from Vredefort Dome are analysed in this paper at both outcrop and microscopic scales in order to quantify their character and to provide possible criteria for comparison and distinction of fault- and impact-generated pseudotachylites.

2. Methods

The Vredefort Dome, located in the central part of the Witwatersrand Basin in South Africa, is now known to be an impact structure. The center of the Vredefort Dome comprises an uplifted granitic basement, which is subdivided into the inner Inlandsee Leucogranofels (ILG) and an outer annulus of Outer Granite Gneiss (OGG) (Stepto, 1990). Pseudotachylites for the clast-size analysis are from Otavi quarry in the OGG, which has been studied in detail by

* Current address: Institute of Experimental Mineralogy, Russian Academy of Sciences, Chernogolovka, Moscow District 142432, Russia.

0191-8141/$ - see front matter © 2004 Elsevier Ltd. All rights reserved.
doi:10.1016/j.jsg.2003.10.007

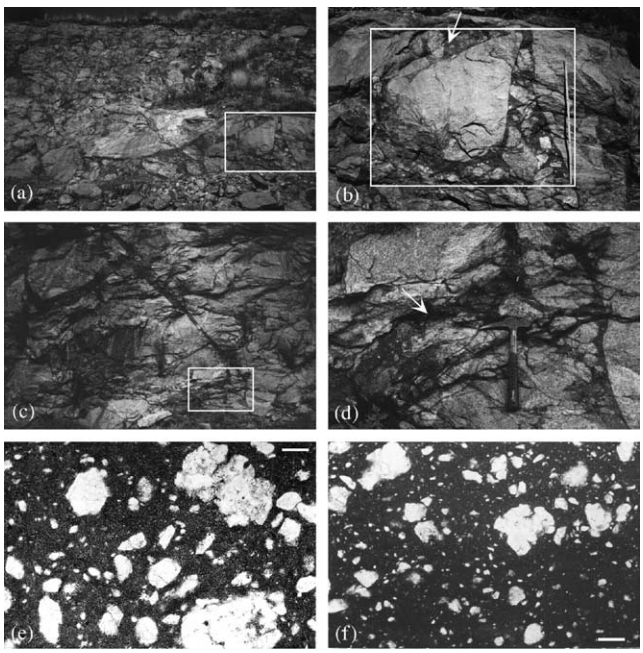

Fig. 1. Pseudotachylites from Otavi quarry in the Vredefort Dome, South Africa. (a) Thick pseudotachylite with many clasts. Square shows the area of (b). (b) Enlarged picture of (a). Square shows the area in which clast-size analysis was conducted. Arrow points to the locality of sample A. Scale bar is 1 m. (c) Pseudotachylite vein, which is about 20 m away from (b). The upper left of the vein connects with the thick pseudotachylite. Square shows the area of (d). (d) Enlarged picture of (c). Arrow points to the locality of sample B. (e) Photomicrograph of sample A. Scale bar is 300 μm. Plane polarized light. (f) Photomicrograph of sample B. Scale bar is 300 μm. Plane polarized light.

many workers (e.g. Bisschoff, 1962; Killick and Reimold, 1990).

The clast-size analyses were conducted on two different scales: outcrop and thin section. To avoid biased measurements, the lengths of the major and minor axes, *a* and *b*, of all clasts within an arbitrarily selected area were measured on each scale. In the outcrop, clast-size distribution analyses were performed on an almost flat surface of the thick pseudotachylite (Fig. 1a and b). For the size of the clasts to be measured, a lower limit of the minor axes of 2.5 mm was set in order to avoid measurement error. For the thin section scale, two samples were studied. One is a sample from the measured outcrop (sample A), and the other is a sample along a vein (sample B) which is about 20 m away from the measured outcrop (Fig. 1c and d). Both samples were examined with three thin sections (A1, A2, A3 and B1, B2, B3). In each thin section, photomicrographs were taken under plane-polarized light (Fig. 1e and f), and the measurements of clast sizes were made on the photomicrographs with a lower limit of the minor axes of 40 μm. Data for the clast-size analysis are summarized in Table 1.

3. Clast-size distribution

It has been widely assumed that when the cumulative number of objects N_c with a characteristic linear dimension greater than r is given by

$$N_c = Cr^{-D} \tag{1}$$

the distribution of objects is a fractal with the fractal dimension D, where C is a constant of proportionality (Turcotte, 1997).

The number of clasts N in certain intervals are cumulated, and N_c is plotted against the mean diameter r, defined as the geometric mean of a and b, using logarithmic scales on both axes (Fig. 2). Because a small number of N_c at the upper end of r may affect the entire trend, $N_c > 10$ is used for the lines of the best fit in Fig. 2. The broken line in Fig. 2a and the solid lines in Fig. 2b and c give the relationship between N_c and r, and their equations are also shown in each figure. It is evident from Fig. 2 that the size distribution of clasts in the pseudotachylite obeys the power-law of the form of Eq. (1) in both outcrop and thin section scales. Although there is only one data set on the outcrop scale, the D-value is expressed as $D = 1.29 \pm 0.02$ with standard error of the slope. On the thin section scale, the mean D-value of three data sets with the 95% confidence limits is calculated as $D = 1.68 \pm 0.22$ for sample A and $D = 1.85 \pm 0.13$ for sample B. Because sample A is from the measured outcrop, by comparison between the two (Fig. 2a and b), it is evident that the D-value at the thin section scale is larger than that at the outcrop scale. On the thin section scale, the D-value of the pseudotachylite vein (sample B) is larger than that of the thick pseudotachylite (sample A) although they are within error of each other.

At the outcrop scale, N_c continues to increase to the lower end of r following the linear relationship (Fig. 2a).

Table 1
Summary of data for the clast-size distribution analysis

Sample	Outcrop	Thin section					
		A1	A2	A3	B1	B2	B3
Approximate area measured	15 m^2	145 mm^2	115 mm^2	90 mm^2	125 mm^2	95 mm^2	95 mm^2
Number of clasts measured	1570	1615	1350	1184	1899	1359	1550
D in the form of Eq. (1)	1.29	1.57	1.79	1.66	1.77	1.89	1.89
Mean $D \pm 2SD$		1.68 ± 0.22			1.85 ± 0.13		

However, on the thin section scale, a slight lower end fall-off from the linear relation is observed in each thin section of both samples (Fig. 2b and c), at a value of r less than about 50 μm. Because the lower limit of the minor axis of 40 μm is large enough on the photomicrographs, it seems that the fall-off is not due to measurement error, but due to melting of fine clasts.

4. Discussion

4.1. Statistical distributions of clasts

Many geological phenomena including frequency–size distributions of rock fragments are considered as scale invariant (e.g. Matsushita, 1985; Mizutani, 1989; Nagahama, 1991). A fractal distribution requires that the number of objects larger than a specified size have a power-law dependence on the size. Because the power-law distribution does not include a characteristic length scale, it must be applicable to scale-invariant phenomena (Turcotte, 1997). Many studies of the number–size distributions of fragments have been carried out, and a variety of statistical power-law relations have often been used as scaling laws (Fujiwara et al., 1977; Sammis et al., 1987; Mizutani, 1989; Mizutani et al., 1990; Nagahama, 1991). Turcotte (1986) demonstrated that the D-value is a measure of the fracture resistance of the material relative to the process causing fragmentation and shows a wide range ($D = 1.44 \sim 3.54$) for a variety of fragmented materials. Although the real geological significance of fractal dimension is unclear, the wide range of D-values represents a variety of deformation modes dependent on geological conditions of deformation (Zhao et al., 1990).

The size distribution of clasts in this study obeys the power-law of the form of Eq. (1) on both outcrop and thin section scales. As D-values in Fig. 2a and b are different beyond the error, however, the distribution is not really scale invariant in the wide range of size. The small D-value on the outcrop scale may imply that the number of big clasts is relatively large. On the thin section scale, D-values of the impact-generated pseudotachylite ($D = 1.68 \pm 0.22$ and 1.85 ± 0.13) may be slightly larger than that of pseudotachylites ($D = 1.5$) in a felsic granulite without a distinct cataclastic fault zone studied by Shimamoto and Nagahama (1992), and that of fault gouge ($D = 1.60$) in the felsic gneiss studied by Sammis et al. (1987) although these values are within error of sample A.

4.2. Fractal limits of clasts

Shimamoto and Nagahama (1992) analysed samples collected from the eastern Musgrave Range, central Australia and empirically presented a power-law with the form of Eq. (1). Nagahama et al. (1994) reconsidered the size distribution of clasts in pseudotachylites from three

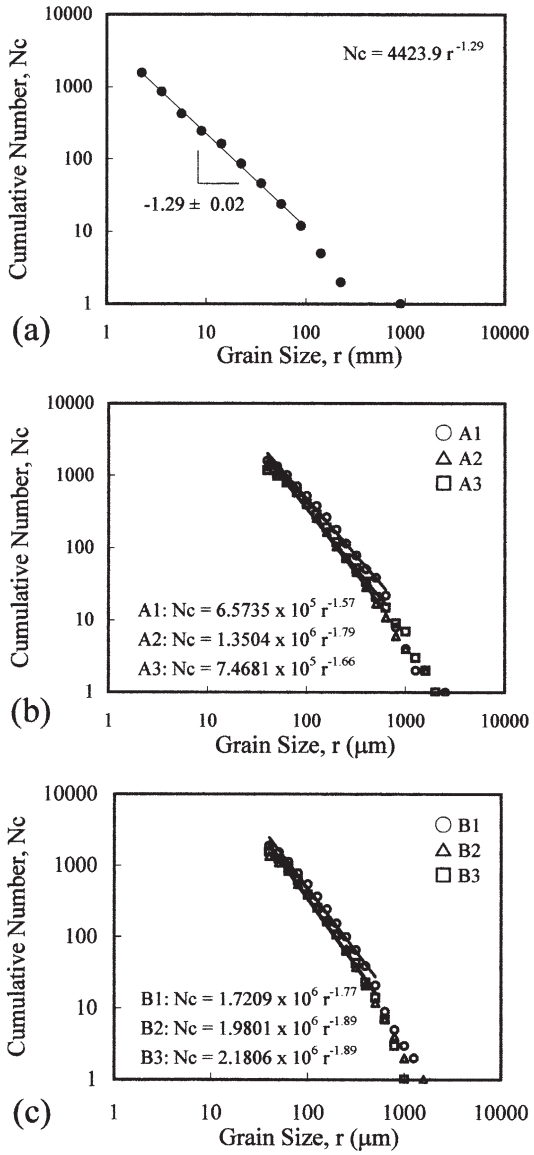

Fig. 2. Cumulative frequency of clast-size in the pseudotachylite from Otavi quarry in the Vredefort Dome, South Africa. Equations are for best fitting lines to the data for $N_c > 10$, which have the power-law of the form of Eq. (1). (a) Measurements on the outcrop. The number of clasts N in intervals of $\log(r) = 0.2$ are counted and cumulated. Standard error of the slope is also shown. (b) Measurements on the thin sections of sample A. The number of clasts N in intervals of $\log(r) = 0.1$ are counted and cumulated. Circles, squares and triangles indicate the data of A1, A2 and A3, respectively. (c) Measurements on the thin sections of sample B. The number of clasts N in intervals of $\log(r) = 0.1$ are counted and cumulated. Circles, squares and triangles indicate the data of B1, B2 and B3, respectively.

different shear zones including the Australian sample with a view to examining the existence of a lower bound for the grain size during the grinding processes. They presented a modified power-law distribution, which can be written as:

$$N_c = N'(1 + r/r')^{-D'} \quad (2)$$

where N' is a total number of clasts and r' and D' are constants. This describes very well the size distribution of

the clasts for the entire range of their size. The size distribution of clasts in natural pseudotachylites has a lower fractal limit around 10–100 μm (fig. 7 in Shimamoto and Nagahama, 1992; fig. 1 in Nagahama et al., 1994). The size distribution of clasts in the experimentally produced pseudotachylite also obeys a power-law of the form of Eq. (2) and has a lower fractal limit around 10 μm (fig. 2 in Tsutsumi, 1999).

In this study, the lower fractal limit is not recognized clearly in Fig. 2, and data of still smaller size are needed. However, the lower end fall-off from the linear relation around $r = 50$ μm may suggest the lower fractal limit, which is on the same order as that of fault-generated pseudotachylites.

Sammis et al. (1987) and Sammis and Biegel (1989) measured the size distribution of rock fragments obtained from the Lopez Canyon Fault, San Gabriel Mountains, California. Although the D-value obtained using their methods cannot be compared directly with this study, as small fragments are usually used in the size distribution studies, data in Sammis and Biegel (1989) that extended the distribution to fragments with diameters up to 410 mm, are relevant to the present study. They sorted the particles into four classes at each scale and calculated the D-value as:

$$D = \frac{\log\left(\frac{N(n)}{A}\right)}{\log\left(\frac{1}{L(n)}\right)} \tag{3}$$

where $N(n)/A$ is the number of particles per unit area and $L(n)$ is the mean diameter of particles in the class n. They showed that $D = 1.60$ in two-dimensional cross-section on scales from 5 μm to 10 mm. They considered the scaled particle density, $N_a(n)$, which is the number of particles in an area scaled to the mean particle dimension, defined as:

$$N_a(n) = \frac{N(n)(L(n))^2}{A} \tag{4}$$

They found that $N_a(n)$ decreases significantly for particles larger than about 10 mm and identified this abrupt decrease in $N_a(n)$ as the upper fractal limit of the gouge (Sammis and Biegel, 1989).

Data in Sammis and Biegel (1989) can be plotted in a $N(n)/A$ vs. $L(n)$ diagram (Fig. 3). In spite of their upper fractal limit, the D-value can be calculated by Eq. (3). The D-value of the in situ data with large diameter is slightly smaller than that of the previous data with small diameter. In the present study, the D-value at the outcrop scale is also smaller than that at the thin section scale (Fig. 2).

Mizutani (1989) summarized experimental studies of impact using a projectile and basaltic targets. The normalized mass of the fragments, m/M_t, where m is the mass of fragments and M_t is the original mass of the target, ranges from 10^{-6} to 1 (Mizutani et al., 1990). If the range is divided into three, each part can be expressed by a linear equation (fig. 2 in Mizutani, 1989; fig. 4 in Mizutani et al., 1990). As

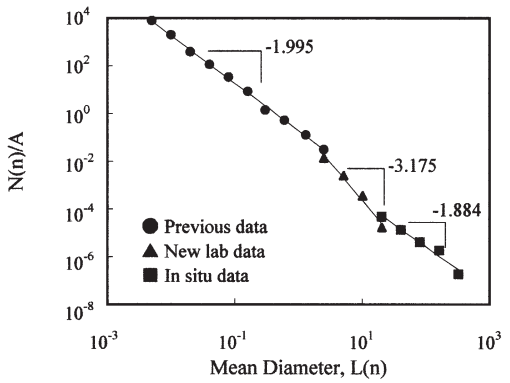

Fig. 3. Log$N(n)/A$ vs. log$L(n)$ diagram with the data from Sammis and Biegel (1989). Sammis et al. (1987) determined the fractal dimension from the slope of least-squares straight line fits in such diagrams. Previous data are microscopic determinations from Sammis et al. (1987). Lab data are new microscopic measurements from large mouldings. In situ data are field determinations. Slopes of each data are also shown.

seen in the present study, the distribution is scale invariant in the limited ranges but not over the entire size range. In the smaller size range ($m/M_t < 10^{-3}$), each experiment yields the same fractal dimension. In the larger size ranges ($m/M_t > 10^{-3}$), however, the fractal dimensions are different and related to the intensity of impact, that is, the more intense impact has the larger fractal dimension. Intensity of impact in the experiments is related to the geometrical configurations of the impact (Fujiwara et al., 1977). If the target is sufficiently large compared with the projectile, the relative intensity is regarded as low. It is interesting to see in the figures of Mizutani (1989) and Mizutani et al. (1990) that when the intensity is low, the D-value in the larger size range is smaller than that in the smaller size range, as seen in the present study, because the size of the largest fragments is very large. Strictly speaking, all clasts in the area from which the clasts might be transported should be measured as in the impact experiment. In the present study, however, as compared with the entire pseudotachylite, only a small part was measured including the outcrop scale. Nevertheless D-values of the impact-generated pseudotachylite in the present study show the trend similar to the impact experiment with low intensity. Among the impact experiment, the one with low intensity may be able to correspond to the phenomenon of a large meteorite impact.

4.3. Proportion of clasts

Schwarzman et al. (1983) studied many pseudotachylites in Vredefort and summarized the textural characteristics of them. According to their study, the pseudotachylites in the OGG have 15–40% of clasts. Spray (1993) reported the volume fraction of clasts for eight unrelated pseudotachylites including two impact-generated pseudotachylites (one of them is with the data from Schwarzman et al. (1983)) and two artificial pseudotachylites. The volume fraction ϕ is

Table 2
Summary of data for the proportion of clasts analysis

Sample	Outcrop	Thin section					
		A1	A2	A3	B1	B2	B3
Approximate area measured	15 m^2	300 mm^2	400 mm^2	360 mm^2	200 mm^2	250 mm^2	220 mm^2
Number of points counted	1308	3017	3915	3451	2164	2586	2102
Proportion of clasts	0.75	0.40	0.39	0.43	0.31	0.37	0.26
Mean proportion of clasts ± 2SD		0.41 ± 0.04			0.32 ± 0.11		

defined as:

$$\phi = V_c/V_t \quad (5)$$

where V_c is the volume occupied by clasts and V_t is the total volume consisting of clasts and matrix. The eight ϕ values have a range from 0.08 to 0.3, and the impact-generated pseudotachylites have the largest and second largest ϕ values ($\phi = 0.3$ for Vredefort and $\phi = 0.25$ for Sudbury).

In the present study, the proportion of clasts was measured using a point-counting technique. Data are summarized in Table 2. The proportion of clasts was calculated as 0.41 ± 0.04 in sample A and 0.32 ± 0.11 in sample B. The errors were determined in each sample as the 95% confidence limits. These proportions of clasts are of the same order as Schwarzman et al.'s (1983) data, and the mean proportion of clasts in the thick pseudotachylite (sample A) may be larger than that in the pseudotachylite vein (sample B) although the mean proportion of clasts in sample B has quite a large error. It has been suggested that the proportion of clasts in the pseudotachylite veins should be lower because of a screening effect of the openings (Ray, 1999). Sample B may be affected by such an effect.

On a large scale, it seems that the proportion of clasts is larger than that in thin sections (Fig. 1a and b). The proportion of clasts in the same area of the clast-size analysis at outcrop was also measured by a point-counting technique on an enlarged photograph Fig. 1b. The proportion of clasts was calculated as 0.75, which is a minimum value because small clasts may have been counted as matrix. This large proportion of clasts, especially on a large scale, may be characteristic of the impact-generated pseudotachylite.

O'Hara (2001) provided a new technique for estimating the ambient crustal temperature during frictional melting, using the ratio of clasts to matrix in the pseudotachylites. According to him, this technique should only be applied to the fault-generated pseudotachylites, in which the clasts can be reasonably interpreted as having been derived from the adjacent walls under adiabatic conditions. As he mentioned, however, the situation for the impact-generated pseudotachylites cannot be regarded as adiabatic because the melt has travelled some distance from the source. Therefore, his technique should not be applied to the present data.

5. Conclusions

Clast-size distribution of impact-generated pseudotachylite has linear relationships for $\log(N_c)$ vs. $\log(r)$ at both outcrop and thin section scales. At the thin section scale, D-values ($D = 1.68 \pm 0.22$ and 1.85 ± 0.13) of the impact-generated pseudotachylite may be slightly larger than those of fault-generated pseudotachylites and fault gouge. As the D-value ($D = 1.29 \pm 0.02$) at the outcrop scale is smaller than that at the thin section scale, however, the distribution is not really scale invariant in the entire range of sizes. On the outcrop scale, N_c continues to increase to the lower end of r, following a linear relationship, but on the thin section scale, the slight fall-off around 50 μm is observed. This fall-off may result from melting of fine clasts and may suggest a lower fractal limit, which is of the same order as that for fault-generated pseudotachylites. Although it is difficult to distinguish impact- and fault-generated pseudotachylites by their fractal dimensions, there is a difference in the proportion of clasts between the two. On the thin section scale, the proportion of clasts for impact-generated pseudotachylites is larger than that for fault-generated pseudotachylites. On the outcrop scale, the impact-generated pseudotachylite has a remarkably high proportion of clasts of at least 0.75, which may be characteristic of the impact-generated pseudotachylite.

Acknowledgements

I greatly thank my colleague, Dr K. Hisada, for his overall cooperation. Prof. W.U. Reimold at the University of the Witwatersrand kindly showed me the field locality, and Prof. T. Shimamoto at Kyoto University gave me a suggestion at the beginning of this study. I would like to thank both of them. I wish to thank Dr T.G. Blenkinsop and two anonymous reviewers for their reviews and improvement of the manuscript. The staff of the Department of Geology at the Rand Afrikaans University and Hiroshima University are also thanked for the use of facilities for this research. Part of this work was financially supported by the JSPS Research Fellowship for Young Scientists.

References

Bisschoff, A.A., 1962. The pseudotachylite of the Vredefort dome. Transactions of the Geological Society of South Africa 65, 207–226.

Dence, M.R., Grieve, R.A.F., Robertson, P.B., 1977. Terrestrial impact structures: principal characteristics and energy considerations. In: Roddy, D.J., Pepin, R.O., Merrill, R.B. (Eds.), Impact and Explosion Cratering. Pergamon Press, New York, pp. 247–275.

Fujiwara, A., Kamimoto, G., Tsukamoto, A., 1977. Destruction of basaltic bodies by high-velocity impact. Icarus 31, 277–288.

Killick, A.M., Reimold, W.U., 1990. Review of the pseudotachylites in and around the Vredefort 'Dome', South Africa. South African Journal of Geology 93, 350–365.

Lambert, P., 1981. Breccia dikes: geological constraints on the formation of complex craters. In: Schultz, P.H., Merrill, R.B. (Eds.), Multi-ring Basins. Proceedings of Lunar and Planetary Science, 12A, pp. 59–78.

Matsushita, M., 1985. Fractal viewpoint of fracture and accretion. Journal of the Physical Society of Japan 54, 857–860.

Mizutani, H., 1989. Size distribution of particles produced at rock fracture. Journal of Geography 98, 696–702. (in Japanese).

Mizutani, H., Takagi, Y., Kawakami, S., 1990. New scaling laws on impact fragmentation. Icarus 87, 307–326.

Nagahama, H., 1991. Fracturing in the solid earth. Science Reports of the Tohoku University. (Geology) 61, 103–126.

Nagahama, H., Shimamoto, T., Ohtomo, Y., Lochhead, A., 1994. Further analysis of clast-size distribution in pseudotachylytes: implications for the origin of pseudotachylyte. Journal of the Tectonic Research Group of Japan 39, 43–49. (in Japanese with English abstract).

O'Hara, K.D., 2001. A pseudotachylyte geothermometer. Journal of Structural Geology 23, 1345–1357.

Okamoto, Y., Kitamura, M., 1994. Melting process of pseudotachylite in granitic gneiss from northwest Scotland. Journal of the Tectonic Research Group of Japan 39, 35–41. (in Japanese with English abstract).

Passchier, C.W., 1982. Pseudotachylyte and the development of ultramylonite bands in the Saint-Barthélemy Massif, French Pyrenees. Journal of Structural Geology 4, 69–79.

Ray, S.K., 1999. Transformation of cataclastically deformed rocks to pseudotachylyte by pervasion of frictional melt: inferences from clast-size analysis. Tectonophysics 301, 283–304.

Reimold, W.U., 1995. Pseudotachylite in impact structures—generation by friction melting and shock brecciation?: a review and discussion. Earth-Science Reviews 39, 247–265.

Reimold, W.U., 1998. Exogenic and endogenic breccias: a discussion of major problematics. Earth-Science Reviews 43, 25–47.

Reimold, W.U., Oskierski, W., Huth, J., 1987. The pseudotachylite from Champagnac in the Rochechouart meteorite crater, France. Journal of Geophysical Research 92, E737–E748.

Sammis, C.G., Biegel, R.L., 1989. Fractals, fault-gouge, and friction. Pure and Applied Geophysics 131, 255–271.

Sammis, C.G., King, G., Biegel, R., 1987. The kinematics of gouge deformation. Pure and Applied Geophysics 125, 777–812.

Schwarzman, E.C., Meyer, C.E., Wilshire, H.G., 1983. Pseudotachylite from the Vredefort Ring, South Africa, and the origins of some lunar breccias. Geological Society of America Bulletin 94, 926–935.

Shimamoto, T., Nagahama, H., 1992. An argument against the crush origin of pseudotachylytes based on the analysis of clast-size distribution. Journal of Structural Geology 14, 999–1006.

Sibson, R.H., 1975. Generation of pseudotachylyte by ancient seismic faulting. Geophysical Journal of Royal Astronomical Society 43, 775–794.

Spray, J.G., 1993. Viscosity determinations of some frictionally generated silicate melts: implications for fault zone rheology at high strain rates. Journal of Geophysical Research 98, 8053–8068.

Spray, J.G., Thompson, L.M., 1995. Friction melt distribution in a multi-ring impact basin. Nature 373, 130–132.

Stepto, D., 1990. The geology and gravity field in the central core of the Vredefort structure. Tectonophysics 171, 75–103.

Thompson, L.M., Spray, J.G., 1994. Pseudotachylytic rock distribution and genesis within the Sudbury impact structure. In: Dressler, B.O., Grieve, R.A.F., Sharpton, V.L. (Eds.), Large Meteorite Impacts and Planetary Evolution. Geological Society of America Special Paper 293, pp. 275–287.

Tsutsumi, A., 1999. Size distribution of clasts in experimentally produced pseudotachylytes. Journal of Structural Geology 21, 305–312.

Turcotte, D.L., 1986. Fractals and fragmentation. Journal of Geophysical Research 91, 1921–1926.

Turcotte, D.L., 1997. Fractals and Chaos in Geology and Geophysics. Cambridge University Press, New York.

Zhao, Z.Y., Wang, Y., Liu, X.H., 1990. Fractal analysis applied to cataclastic rocks. Tectonophysics 178, 373–377.